Characterization of the Nonlinear Elastic Properties of Graphite/Epoxy Composites Using Ultrasound

William H. Prosser and Robert E. Green, Jr.

Journal of Reinforced Plastics and Composites, Vol. 9,
March 1990, pp. 162-173

ABSTRACT

The normalized change in ultrasonic "natural" velocity as a function of stress and temperature was measured in a unidirectional laminate of T300/5208 graphite/epoxy composite using a pulsed phase locked loop ultrasonic interferometer. These measurements were used together with the linear (second order) elastic moduli to calculate some of the nonlinear (third order) moduli of this material.

INTRODUCTION

Nonlinear elastic moduli are important physical properties in conventional materials. They provide information about the interatomic bonding forces in crystalline solids. Nonlinear properties are also important in the nondestructive determination of applied and residual stress (strain) and several investigations have also established a possible relationship between nonlinear elastic properties and ultimate strength in aluminum and carbon steel [1,2]. Conventional mechanical testing does not have sufficient sensitivity to measure the nonlinearity in the mechanical behavior in most materials. However, the effects of nonlinear elasticity on elastic wave propagation such as harmonic generation, elastic wave interaction, and velocity dependence on applied stress or temperature can be used to characterize these properties.

In this research, an effort was made to determine the nonlinear elastic moduli of a unidirectional T300/5208 graphite/epoxy composite. This was accomplished by first determining the linear elastic moduli by both strain gage measurements during quasi-static uniaxial loading and ultrasonic velocity measurements. The stress and temperature dependence of the ultrasonic "natural" velocity was measured using a pulsed phase locked loop interferometer. Equations were derived to relate the stress dependence

---

William H. Prosser, NASA Langley Research Center, Mail Stop 231, Hampton, VA. 23665.
Robert E. Green, Jr., Center for Nondestructive Evaluation, Johns Hopkins University, Baltimore, MD. 21218.

*This work was partially supported by NASA Training Grant NGT 21-001-802. A special note of thanks in this regard is due Dr. Joseph S. Heyman, NASA Langley Research Center.

of the velocity, and the linear elastic moduli to the nonlinear elastic moduli. In addition, a least squares method was applied to calculate a best fit for the nonlinear moduli from the measured data. Although unidirectional composites are most often characterized as transversely isotropic materials, the measured linear and nonlinear elastic properties exhibited small deviations from this transversely isotropic behavior. Thus, the nonlinear moduli were calculated for models of transversely isotropic and orthotropic elastic symmetry.

LINEAR (SECOND ORDER) ELASTIC PROPERTIES

The material used in this study was cut from a thick (0.8 in.) unidirectional laminate of T300/5208 graphite/epoxy. The original laminate was ultrasonically C-scanned for gross voids and defects. None were found to be present.

The linear elastic stiffness moduli were calculated from measurements of the density and ultrasonic wave speeds at 2.25 MHz. Although these measurements would have ideally been made on a single specimen to avoid any errors due to sample to sample variations, the large attenuation of shear mode waves necessitated the use of several specimen. The dimensions and densities of these samples are given in Table 1. The longitudinal measurements were made on sample 1.10A while the shear wave measurements were made on the other three. The equations used for these calculations were similar to those presented by Kriz and Stinchcomb [3] for a transversely isotropic composite material. However, in this work, the fiber axis was designated as the x_3 direction as indicated by Fig. 1. The ultrasonic measurements demonstrated deviations from transversely isotropic behavior. Therefore, the stiffness moduli were also calculated using orthotropy as the elastic symmetry model. The stiffness moduli for this material for both the transversely isotropic and orthotropic symmetry models are presented in Table 2. The large uncertainties in the c_{13} and c_{23} moduli are due to the large uncertainties in the velocity measurements of the off axis non-pure mode waves needed to calculate these moduli. These measurements were made on specimens cut with the direction of propagation 45 degrees between the x_1 and x_3 axes.

The linear elastic compliance moduli were determined using strain gage measurements and uniaxial compressive quasi-static loading. The measured moduli are presented in Table 3. Again, there was a small deviation from transversely isotropic behavior. The stiffness moduli were inverted and compared with the compliance moduli and were found to be in good agreement.

NONLINEAR (THIRD ORDER) ELASTIC PROPERTIES

Using the linear elastic stiffness and compliance moduli, the nonlinear elastic moduli can be calculated from measurements of the stress dependence of the ultrasonic "natural" velocity. The "natural" velocity (W) was defined by Thurston and Brugger [4] as the velocity referred to the unstressed or natural state. It is given by

$$W = \frac{L_0}{t} \quad , \tag{1}$$

where L_0 is the specimen length in the natural or unstressed state and t is the time of flight of the ultrasonic wave. Since L_0 is a constant, the normalized change of "natural" velocity with respect to a change in

temperature or stress is given by

$$\frac{\Delta W}{W} = -\frac{\Delta t}{t} \quad . \tag{2}$$

Thus, only the change in time of flight of the ultrasonic wave need be measured.

In these measurements however, a pulsed phase locked loop (P2L2) ultrasonic interferometer was used to measure changes in "natural" velocity at frequencies near 2.25 MHz. This instrument, developed by Heyman [5], is shown schematically in Fig. 2. The heart of the P2L2 is a voltage controlled oscillator (VCO) which generates a continuous wave signal of a frequency that is controlled by a D.C. input signal. A portion of the signal from the VCO is gated out into a tone burst and is then used to excite the ultrasonic transducer. The resulting elastic wave is launched into the sample and is then detected either by the same transducer in the pulse echo mode or another transducer in the through transmission mode. The received signal is input into the P2L2 where it is phase compared with the signal from the VCO at a preselected phase point using a sample and hold. The sampled voltage from the phase detector is then used to drive the VCO to a condition of quadrature. The acoustic phase shift (θ) given by

$$\theta = 2\pi ft \tag{3}$$

where f is the frequency, is then maintained as a constant by the feedback loop and therefore

$$\Delta\theta = 0 = 2\pi(t\Delta f + f\Delta t) \quad . \tag{4}$$

Combining equations (3) and (4) yields

$$\frac{\Delta\theta}{\theta} = 0 = \frac{\Delta f}{f} + \frac{\Delta t}{t} \tag{5}$$

and thus,

$$\frac{\Delta f}{f} = -\frac{\Delta t}{t} = \frac{\Delta W}{W} \quad . \tag{6}$$

By monitoring the normalized change of frequency of the P2L2, the normalized change in "natural" velocity is determined.

The measurements made in this work were of the Stress Acoustic Constants (SAC) and the Thermal Acoustic Constants (TAC). The Stress Acoustic Constant, as defined by Heyman [2] and Cantrell [6] is given by

$$H = \frac{\frac{\Delta W}{W}}{\Delta\sigma} = \frac{\frac{\Delta f}{f}}{\Delta\sigma} \tag{7}$$

where σ is the applied stress which is either hydrostatic or uniaxial. The SAC's were measured for twenty seven combinations of stress, direction of propagation and polarization of the ultrasonic wave. To differentiate between these, each SAC is given three subscripts. The first represents the direction of applied stress which was limited to being along one of the three coordinate axes. A 0 for this subscript implies that the loading was hydrostatic. The second subscript gives the direction of propagation and

the third gives the polarization direction. These were also limited to being pure mode waves along the three coordinate axes. The direction of propagation was always perpendicular to the direction of loading for the uniaxial SAC measurements which were made under compression. The same specimen that were previously described were used for these measurements.

During the uniaxial SAC measurements, the specimen were loaded to between 80 and 100 MPa. The loading rate was varied considerably (25 to 500 MPa/Min.) to determine its effect on the measured velocity changes. Within this range there was no measured effect indicating that viscoelastic effects were negligible. Each uniaxial SAC value was determined from the average of ten measurements during which the transducer was rebonded to the sample several times. Although most of the measurements demonstrated linear relationships between normalized frequency shift and stress, several exhibited nonlinear (quadratic) behavior. These were fit to a quadratic fit with the SAC value taken as the linear term of this fit. The measured values for the uniaxial SAC's are shown in Table 4 with those which were quadratic designated by an *. Typical curves for two of the uniaxial measurements are shown in Figs. 3 and 4. A block diagram of the experimental apparatus is shown in Fig. 5.

The hydrostatic SAC measurements were made in a similar fashion except that the pressure chamber was limited to a maximum of 250 psi. This was about a factor of fifty lower than the uniaxial maximum stress. This much lower pressure produced smaller velocity changes making these measurements much more uncertain. This limitation in pressure also made the measurement of H_{033} impossible because the changes involved were too small to be detected with the P2L2. The measurements also had to be made over long periods of time to avoid temperature variations caused by increasing the pressure of the Argon gas in the chamber. Because of the long length of time required to make each measurement only three measurements were averaged for each hydrostatic SAC value. The results are presented in Table 4 with a typical curve shown in Fig. 6. The block diagram of the measurement system is shown in Fig. 7. For these small pressure changes, the relationships were all linear.

The effect of temperature on the "natural" velocity was also measured for small variations about room temperature. The apparatus used for these measurements was the same as that used in the hydrostatic measurements. The temperature was increased above room temperature several degrees C in 0.3 C steps using the heaters and temperature controller in the pressure vessel system. The frequency shift was measured at each point after thermal equilibrium was attained. The Thermal Acoustic Constants, defined as

$$H_T = \frac{\frac{\Delta f}{f}}{\Delta T} \qquad (8)$$

where T is temperature, are given in Table 5. The second and third subscripts give the direction of propagation and polarization respectively. They were measured for nine combinations of propagation direction and polarization. The curves all exhibited linear relationships.

The Stress Acoustic data was used to determine some of the nonlinear elastic moduli for this material. Since the linear elastic moduli and the SAC data exhibited small deviations from transversely isotropic behavior, the moduli were calculated for both the transversely isotropic and orthotropic elastic symmetry models. For the case of transverse isotropy,

there are nine independent third order moduli while for orthotropy there are twenty. However, because H_{033} was unable to be determined, several of the moduli could not be calculated. The transversely isotropic c_{133} and c_{333} and the orthotropic c_{133} , c_{233} , c_{333} , c_{123} , and c_{456} could not be determined.

The theoretical basis for these calculations comes from the work of Thurston and Brugger [4] who presented generalized equation for the derivative of the "natural" velocity with respect to stress evaluated at zero stress ($(\rho_0 W^2)'_{p=0}$). These equations were written in terms of the unstressed density (ρ_0), the adiabatic linear elastic stiffness moduli (c^S_{ijkl}), the isothermal linear elastic compliance moduli (s^T_{ijkl}), and the third order elastic stiffness moduli (c_{ijklmn}). For the case of hydrostatic pressure the equation was

$$- (\rho_0 W^2)'_{p=0} = 1 + 2wF_{HC} + G_{HC} \qquad (9)$$

where

$$w = (\rho_0 W^2)_{p=0} = c^S_{prqs} N_p N_q U_r U_s \ , \qquad (10)$$

$$F_{HC} = s^T_{aars} U_r U_s \ , \qquad (11)$$

and

$$G_{HC} = s^T_{aauv} c_{uvprqs} N_p N_q U_r U_s \ . \qquad (12)$$

N_i and U_i are the direction cosines of the directions of polarization and particle displacements referred to the "natural" state. The summation convention on repeated indices is assumed throughout this paper. For uniaxial stress, the equation becomes

$$- (\rho_0 W^2)'_{p=0} = 2wF_{UC} + G_{UC} \ , \qquad (13)$$

where

$$F_{UC} = s^{T}_{abrs} M_a M_b U_r U_s \ , \tag{14}$$

$$G_{UC} = s^{T}_{abuv} c_{uvprqs} M_a M_b N_p N_q U_r U_s \ , \tag{15}$$

and M_i are the components of a unit vector in the direction of stress which is always perpendicular to the direction of propagation of the ultrasonic wave. The relationship between these equations and the SAC is given by

$$H = \frac{(\rho_0 W^2)'_{p=0}}{(2\rho_0 W^2)} \ . \tag{16}$$

Thus, a system of equations can be derived for the models of transverse isotropy and orthotropy that relate the measured linear elastic moduli and SAC's to the unknown third order elastic coefficients. These equations, although too lengthy for presentation here, were presented by Prosser [7].

A least squares procedure as outlined by Hankey and Schuele [8], was used to reduce the data and determine a best fit for the values of the nonlinear coefficients. This was done for both the transversely isotropic and orthotropic elastic symmetry models. The results of this reduction with the estimated maximum and probable limits of error are shown in Table 6. The values are all negative with the exception of c_{123}. This is in agreement with the nonlinear behavior of conventional materials. The large uncertainties in some of the moduli arise from the large uncertainty of the hydrostatic SAC measurements. These large uncertainties mask any deviations from transversely isotropic behavior in the third order elastic coefficients within the uncertainty of the calculations.

SUMMARY AND CONCLUSIONS

This research provides initial measurements of the characterization of the nonlinear elastic properties of graphite/epoxy composites using ultrasound.

These will provide the basis for studying the relationships between nonlinear properties and more important engineering properties such as ultimate strength, residual strength after impact and fatigue loading, and fiber-matrix interfacial strength. These measurements also serve as a basis for a study into the ultrasonic measurement of residual stress (strain) in graphite/epoxy composites which may arise because of the mismatch in coefficients of thermal expansion of fiber and matrix. Thus, these measurements of the nonlinear properties may aid in the development of needed nondestructive evaluation techniques for graphite/epoxy composites. However, from a practical standpoint, the measured SAC's values are probably more useful than the calculated nonlinear moduli. This is because they are more easily obtained with smaller experimental uncertainty and can be measured in an individual specimen instead of calculated from measurements made in several specimen. Also, the SAC's are the quantities that are more useful in experimental attempts to measure applied and residual stress and may be important in nondestructive evaluation of ultimate strength of materials.

REFERENCES

1. Heyman, J. S., and Chern E. J., "Characterization of Heat Treatment in Aluminum Based on Ultrasonic Determination of the Second and Third Order Elastic Constants," IEEE Ultrasonics Symposium, 1981, pp. 936-939.

2. Heyman, J. S., Allison, S. G., and Salama, K., "Influence of Carbon Content on Higher-Order Ultrasonic Properties in Steels," IEEE Ultrasonics Symposium, 1983, pp. 991-994.

3. Kriz, R. D., and Stinchomb, W. W., "Elastic Moduli of Transversely Isotropic Graphite Fibers and their Composites," Experimental Mechanics, Vol. 19, 1979, pp. 41-49.

4. Thurston, R. N., and Brugger, K., "Third-Order Elastic Constants and the Velocity of Small Amplitude Elastic Waves in Homogeneously Stressed Media," Physical Review, Vol. 133, 1966, pp. A1604-A1610.

5. Heyman, J. S., "Pulsed Phase Locked Loop Strain Monitor," NASA Patent

Disclosure LAR 12772-1, 1980.

6. Cantrell, J. H., Jr., "Anharmonic Properties of Solids from Measurements of the Stress Acoustic Constant," Journal of Testing and Evaluation, Vol. 10, 1982, pp. 223-229.

7. Prosser, W. H., Master's Essay, Johns Hopkins University, 1987, pp. 81-84.

8. Hankey, R. E., and Schuele, D. E., "Third Order Elastic Coefficients of Al_2O_3," Journal of the Acoustical Society of America, Vol. 48, 1970, pp. 190-202.

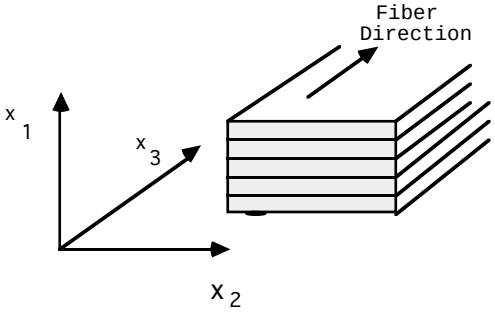

Fig. 1. Illustration of axis designation in a unidirectional composite with respect to fiber direction.

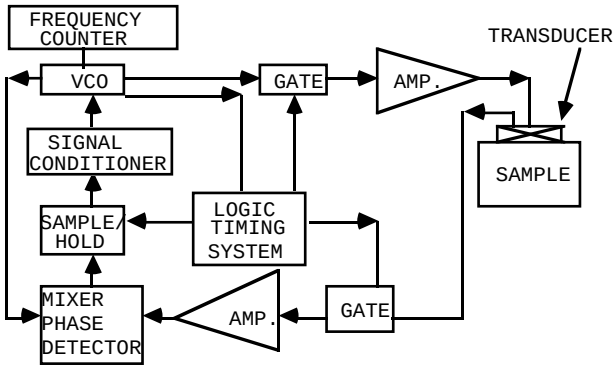

Fig. 2. Block diagram of the pulsed phase locked loop ultrasonic interferometer.

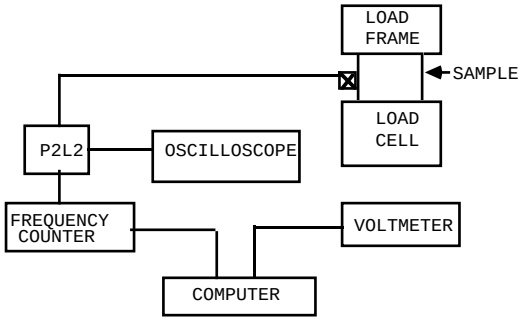

Fig. 5. Block diagram of uniaxial stress acoustic constant measurement apparatus.

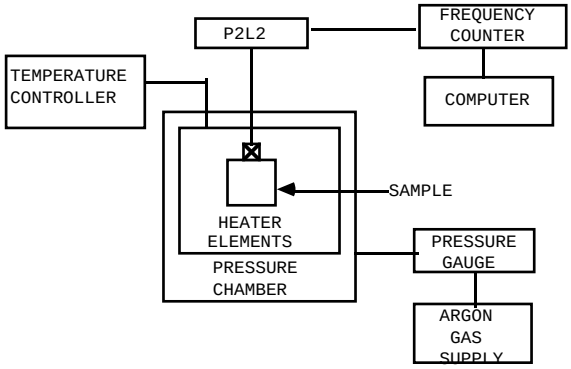

Fig. 7. Block diagram of hydrostatic stress acoustic and thermal acoustic constant apparatus.

Table 1 - Sample dimensions and densities

Sample Number	Dimensions (in.) x_1	x_2	x_3	Density (g/cm^3)
1.10A	0.8001	0.7999	0.8002	1.5404 +/- 0.0004
1.10B	0.7999	0.5002	0.7996	1.5460 +/- 0.0006
1.8A	0.8002	0.8000	0.5002	1.5384 +/- 0.0005
1.7A	0.5001	0.8001	0.7999	1.5411 +/- 0.0005

Table 2 - Linear Elastic Stiffness Moduli

Transverse Isotropy	Value (GPa)	Orthotropy	Value (GPa)
c_{11}	14.26	c_{11}	14.295
c_{12}	6.78	c_{12}	6.78
c_{13}	3.0 - 8.9	c_{13}	3.3 - 9.0

Table 2 - Continued

Transverse Isotropy	Value (GPa)	Orthotropy	Value (GPa)
c_{33}	108.4	c_{33}	108.4
c_{44}	5.27	c_{44}	5.28
		c_{55}	5.27
		c_{66}	3.74
		c_{22}	14.226
		c_{23}	6.6 - 7.7

Table 3 - Linear elastic compliance moduli

Transverse	Value$(GPa)^{-1}$	Orthotropy	Value $(GPa)^{-1}$
s_{11}	0.089	s_{11}	0.0890
s_{12}	-0.063	s_{12}	-0.0626
s_{13}	-0.0021	s_{13}	-0.00208
s_{33}	0.00935	s_{33}	0.00935
		s_{22}	0.0891
		s_{23}	-0.00215

Table 4 - Stress Acoustic Constants

SAC	Value $(GPa)^{-1}$	SAC	Value $(GPa)^{-1}$	SAC	Value $(GPa)^{-1}$
H_{122}^*	0.0490 +/- 0.0009	H_{211}^*	0.0427 +/- 0.001	H_{322}	0.00116 +/- 0.00007
H_{311}	0.00123 +/- 0.00001	H_{121}	0.0887 +/- 0.0007	H_{212}	0.0741 +/- 0.0010
H_{312}	0.00279 +/- 0.00010	H_{321}	0.00299 +/- 0.00010	H_{123}^*	0.068 +/- 0.002
H_{213}^*	0.0572 +/- 0.0010	H_{323}	-0.00993 +/- 0.0004	H_{313}	-0.00919 +/- 0.0003
H_{131}	0.165 +/- 0.003	H_{232}	0.149 +/- 0.002	H_{132}	0.111 +/- 0.002
H_{231}	0.109 +/- 0.001	H_{133}	0.0538 +/- 0.0005	H_{233}	0.0479 +/- 0.0003

H_{011} 0.39 +/- 0.02	H_{022} 0.37 +/- 0.02	H_{012} 0.257 +/- 0.007
H_{021} 0.261 +/- 0.006	H_{013} 0.27 +/- 0.03	H_{023} 0.27 +/- 0.02
H_{031} 0.28 +/- 0.02	H_{032} 0.25 +/- 0.02	H_{033} Not measured

Table 5 - Thermal Acoustic Constants

TAC	Value (10^{-4} C^{-1})	TAC	Value (10^{-4} C^{-1})	TAC	Value (10^{-4} C^{-1})
H_{T11}	-6.36 +/- 0.02	H_{T22}	-6.33 +/- 0.03	H_{T12}	-8.5 +/- 0.1
H_{T21}	-8.5 +/- 0.01	H_{T13}	-10.2 +/- 0.02	H_{T23}	-10.1 +/- 0.2
H_{T31}	-7.1 +/- 0.5	H_{T32}	-7.6 +/- 0.7	H_{T33}	-0.72 +/- 0.09

Table 6 - Third Order Elastic Moduli

Transverse Isotropy				Orthotropy			
Modulus	Value (GPa)	Maximum Error	Probable Error	Modulus	Value (GPa)	Maximum Error	Probable Error
c_{111}	-214	17	4	c_{111}	-196	15	3
c_{112}	-89	12	3	c_{112}	-94	5	1
c_{113}	-4	110	23	c_{113}	-63	63	13
c_{123}	65	109	23	c_{122}	-91	8	2
c_{144}	-33.4	3	0.5	c_{222}	-186	21	4
c_{155}	-49.1	4	0.8	c_{223}	-60	93	19
c_{344}	-47	30	6	c_{144}	-33.0	2.4	0.5
				c_{244}	-47.8	3.3	0.7
				c_{344}	-46	27	6
				c_{155}	-50.1	3.9	0.8
				c_{255}	-33.5	2.8	0.6

c_{355}	-49	32	7
c_{166}	-33.9	0.6	0.1
c_{266}	-33.1	0.6	0.1
c_{366}	-28.5	4.0	0.8